SPATIO-TEMPORAL DEFECT PIXEL INTERPOLATION USING 3-D FREQUENCY SELECTIVE EXTRAPOLATION

Katrin Meisinger[1], *Til Aach*[2], *and André Kaup*[1]

[1]Multimedia Communications and Signal Processing,
University Erlangen-Nuremberg,
Cauerstr. 7, 91058 Erlangen, Germany.
Email: {meisinger,kaup}@LNT.de

[2]Institute of Imaging and Computer Vision,
RWTH Aachen University
Sommerfeldstr. 24, 52074 Aachen, Germany.
Email:til.aach@lfb.rwth-aachen.de

ABSTRACT

Flat panel X-ray detectors allow the immediate availability of the acquired images for display. However, they provide images with defective areas amongst others due to manufacturing problems. In this contribution, we present a frequency selective extrapolation method in order to restore these defects by extending the surrounding signal into the defective area. In case of static radiographs, the spatial surrounding is evaluated by a 2-D approach. Defects in sequences acquired by cine-angiography or fluoroscopy are processed by 3-D extrapolation. The defects are replaced by extrapolating the signal from the spatial and at the same time temporal surrounding, taking previous and subsequent frames into account. Hence, inherent motion compensation is accomplished. The application of the spatial and where applicable spatio-temporal extrapolation approach allows to restore smooth areas, edges, patterns as well as noise. The ability to restore noise is especially important for medical images because it leads to a natural appearance of the concealed defective areas.

Index Terms—
Signal extrapolation, medical imaging, defect interpolation

1. INTRODUCTION

Clinical X-ray projection imaging is undergoing profound changes with the introduction of large flat panel detector systems [1, 2]. Such solid state detectors consist, for instance, of charge coupled devices (CCDs) optically coupled to an X-ray sensitive screen by fibers or lenses [3]. An alternative design is based on a large array of light sensitive pixels that is manufactured from amorphous silicon (a-Si) [1, 4, 5]. Sensitivity to x radiation is achieved by a coating of thallium-doped cesium-iodide (CsI:Tl). One advantage of solid state flat panel detectors in comparison to conventional radiography is that the acquired X-ray images are almost immediately available for viewing. In addition, there are no recurring film costs per image, the possibility to compensate within certain limits for over- or underexposure, and the possibility of enhancement by digital filtering [1, 6, 7]. Moreover, a-Si flat panel detectors also permit the acquisition of X-ray fluoroscopy. In comparison to classical fluoroscopy detection front ends consisting of an image intensifier (II) optically coupled to a camera [1, 8], the mechanical dimensions and the weight of a flat detector are much lower. Finally, a flat detector avoids geometric distortions introduced by the generally convex entrance screen of the II, and is free of distortions due to scattering in the II, such as veiling glare.

In practice, large area flat panel detectors may still contain regions with inactive pixels (see e.g. Ref. [2, p. 287]), due to, e.g., the construction of a large detector by tiling four smaller ones. The inactive pixels sites are known from calibration measurements. The corresponding defects in the images can then be interpolated from adjacent pixels. A straightforward approach is nonadaptive linear interpolation. A better reconstruction of, for instance, orientated structures crossing a defect, such as guidewires, catheters or edges of bones, can be achieved by nonlinear interpolation, e.g. by a median filter [2], or by directionally adaptive linear interpolation [9, 10]. These spatial-domain interpolation algorithms include weighted averaging of the intensities surrounding a defect. Therefore, interpolated defects exhibit a different noise structure which may give the radiograph a somewhat unnatural appearance. In addition, they may be unable to cope with more complex structures than single directional image neighbourhoods.

In this paper, we therefore describe an alternative interpolation algorithm that works in the spectral domain. The known signal surrounding the defect is extrapolated into the defective area by evaluating the surrounding iteratively by dominant features in terms of DFT coefficients. In [18] this approach was used in clinical X-ray imaging. Compared to that approach, in [16] a weighting function is introduced which allows a special adaptation of the error criterion to the application with respect to the signal and the shape of the loss. For image signals in error concealment of erroneous image communications the modified error criterion led to better performance at less iterations [16] compared to a binary weighting function [15]. Medical image signals have different properties than image signals because they underly different statistics. They exhibit a large amount of noise. Besides, the shape of the loss in defect pixel interpolation is different compared to concealment in image communications. Due to the frequency selective nature of the algorithm in terms of selected dominant DFT coefficients, in principle smooth areas, edges as well as noise-like structures can be extended into the defective area. Especially the property to restore noise should be exploited in order to lead to a natural appearance of the medical images. This overcomes the drawback of spatial-domain based interpolation algorithms causing blurry artifacts. Further, larger areas can be concealed.

In this contribution for static radiographs, the 2-D extrapolation method is applied by evaluating the spatial surrounding. In case of sequences acquired by fluoroscopy or cine-angiography, the 2-D extrapolation approach is extended to 3-D in order to gain information about the defect from previous and following frames additionally to the spatial surrounding. Hence, we do not only evaluate the spectrum of the spatial surrounding within the image but at the same time the temporal surrounding from previous and following frames. Applying conventional motion compensated techniques known from video coding is difficult due to the large amount of noise in medical images. Additionally, if the noise of the motion compensated block

does not fit to the surrounding, block artifacts at the block boundary occur. In contrast, the noise structure is inherently imitated by spatio-temporal frequency selective extrapolation.

In summary, in this contribution we investigate the application of frequency selective extrapolation to medical image signals in defect pixel interpolation. We evaluate also if a special adaptation of the error criterion is beneficial in this case. Further, by extending the 2-D approach to 3-D for sequences as acquired in cine-angiography information about the defect should be gained from previous and following frames additionally to the spatial surrounding.

2. DEFECT INTERPOLATION BY FREQUENCY SELECTIVE EXTRAPOLATION

The defect is replaced by extrapolating the surrounding image signal into the missing area. For detailed derivations the reader is referred to [14, 16] for the 2-D case and to [17] for the 3-D derivations. Here, the concept of spatio-temporal extrapolation is presented and all implementational issues regarding the medical image signal and the shape of the loss caused by the defects of the panels.

A possible sequence of five frames is shown in Fig. 1. The spatial dimensions are denoted by m, n and the temporal dimension by t. The respective areas which are used for the reconstruction of the defective area are marked by a bold border. The block $\mathcal{B}$ shaded dark gray in image τ within the bold border is to be extrapolated from the area $\mathcal{A}$. The support area $\mathcal{A}$ ranges from two previous to two subsequent frames including the surrounding of the area to be estimated in the actual frame. The defect is present in all frames at the same location. Note, that in case of defect interpolation already restored areas can be taken into account whereas the defect in future frames has to be omitted for estimating the defective area in frame τ. The entire region $\mathcal{L}$ - consisting of the region to be estimated $\mathcal{B}$ and the support area $\mathcal{A}$ - is described by a volume.

The known pixels $f[m, n, t]$ are approximated iteratively by the parametric model $g[m, n, t]$. The spatio-temporal description by $g^{(\nu)}[m, n, t]$ approximates the support area in iteration ν by a linear combination of basis functions $\varphi_{k,l,p}[m, n, t]$ weighted by expansion coefficients $c^{(\nu)}_{k,l,p}$

$$g^{(\nu)}[m, n, t] = \sum_{(k,l,p)\in\mathcal{K}_\nu} c^{(\nu)}_{k,l,p}\ \varphi_{k,l,p}[m, n, t]. \tag{1}$$

The set $\mathcal{K}_\nu$ describes the basis functions used. The basis functions are defined in the entire area $\mathcal{L}$ and its number of basis functions $M \times N \times T$ equals the number of pixels in $\mathcal{L}$. Here, the principle is described for real valued basis functions and expansion coefficients.

In each iteration, the parametric model is updated by a weighted suitable basis function $\varphi_{u,v,q}[m, n, t]$

$$\Delta g = \Delta c \cdot \varphi_{u,v,q}[m, n, t]. \tag{2}$$

As error criterion the error energy between the original signal and its approximation by the parametric model weighted by $w[m, n, t]$ before summation is evaluated with respect to the support area

$$E^{(\nu+1)}_{\mathcal{A}} = \sum_{(m,n,t)\in\mathcal{L}} w[m, n, t] \cdot \Big(f[m, n, t] - g^{(\nu)}[m, n, t] - \Delta c\varphi_{u,v,q}[m, n, t]\Big)^2, \tag{3}$$

where the weighting function $w[m, n, t]$ allows to specially adapt the error criterion to the respective application.

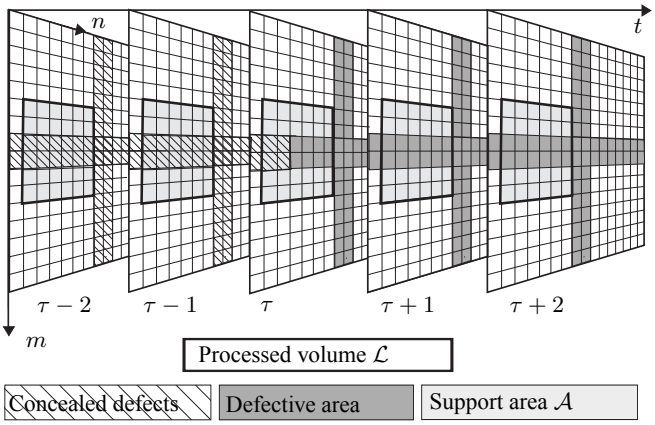

Fig. 1. Image areas used for 3-D extrapolation consisting of the area to be estimated and its known surrounding.

Δc is determined by minimizing the error criterion (3) by taking the derivative with respect to the unknown coefficient and setting it to zero.

The coefficient $c^{(\nu+1)}_{u,v,q}$ is subsequently updated

$$c^{(\nu+1)}_{u,v,q} \quad = \quad c^{(\nu+1)}_{u,v,q} + \Delta c. \tag{4}$$

Per iteration, we choose that basis function $\varphi_{u,v,q}[m, n, t]$ which leads to a maximum reduction of the residual error criterion

$$\Delta E^{(\nu+1)}_{\mathcal{A}} = \sum_{(m,n,t)\in\mathcal{L}} w[m, n, t]\big(\Delta c\varphi_{k,l,p}[m, n, t]\big)^2$$

$$\Longrightarrow (u, v, q) = \arg\max_{(k,l,p)} \Delta E^{(\nu+1)}_{\mathcal{A}}.$$

The index of the selected basis function is included in the set of used basis functions in case it has not been selected yet

$$\mathcal{K}_{\nu+1} = \mathcal{K}_\nu \cup \{u, v, q\} \quad \text{if} \quad (u, v, q) \notin \mathcal{K}_\nu. \tag{5}$$

The algorithm terminates if the reduction of the residual error energy drops below a pre-specified threshold $\Delta E_{\min}$ per pixel.

Summarising the main points of the algorithm, the image content in the spatio-temporal volume is described *simultaneously* in *spatio-temporal* direction by dominant features in terms of weighted basis functions.

The basis functions are defined in the entire volume, therefore each approximation provides at the same time an estimation of the defective samples. Finally, the extrapolated area is cut out of the parametric model.

3-D Discrete Fourier Transform (DFT) basis functions are used for the approximation allowing an efficient realization in the frequency domain using FFT algorithms. Hence, per iteration one DFT coefficient is chosen. The parametric model $g^{(\nu)}[m, n, t]$ in the spatio-temporal volume is then given by the inverse DFT and the defect in frame τ is replaced by cutting the estimated area out of $g^{(\nu)}[m, n, \tau]$.

3. IMPLEMENTATION ASPECTS

The frequency selective extrapolation algorithm is investigated for medical image signals in digital X-ray imaging acquired by flat-panel detectors. Compared to error concealment in image communications the underlying signal exhibits different statistics and the

shape of the loss differs. The defects are detected prior to processing by calibration measurements. Hence, a mask with the locations of the defects is available. Three different error-patterns which occur typically are introduced into processed images. An error grid of 2 pixels simulates the construction of a large detector by putting together quarter panels. Further, inactive pixels typically occurring in clusters and row losses are simulated.

The grid defects are restored sequentially and processed in a block-wise fashion. The defective pixels are surrounded by the support area consisting of 7 pixels in spatial direction forming a block of 16×16 pixels processed by a 2-D FFT of likewise 16×16 in case of 2-D extrapolation. However, only the central block of 2×2 pixels is replaced by the extrapolation result and already replaced defects are taken into account with less weight. Maximally 10 iterations per blocks are done. In defect pixel interpolation, we use an isotropic function in the support area

$$w[m,n,t] = \begin{cases} \hat{\rho}^{\sqrt{\left(m-\frac{M-1}{2}\right)^2+\left(n-\frac{N-1}{2}\right)^2+\left(t-\frac{T-1}{2}\right)^2}}, \\ \qquad\qquad (m,n,t) \in \mathcal{A} \\ 0, \qquad\qquad (m,n,t) \in \mathcal{B} \end{cases}$$

allowing to emphasize regions which are closer to the defect. $\hat{\rho}$ is a prespecified constant with $\hat{\rho} = 0.4$.

Then, the processing window of 16×16 is moved by 2 pixels. The row defects are processed in the same sequential way, there 1×2 pixels per processed block are replaced. The cluster errors are small enough to be replaced at once.

In case of 3-D, the sequential processing procedure remains unchanged. Hence, the support area does not only consist of the spatial surrounding but of a volume including information from one previous and one following frame. The sequences may exhibit strong motion or rotational changes, that is why only one previous and one following frame is taken into account. The same holds for cases where a contrast medium is injected. More information about the defect could be obtained for slowly moving or rotating areas by involving more frames identified by motion analysis. In case of the first frame of the sequence, only the subsequent frame is involved. Similarly, restoring defects in the last frame can be achieved by involving only the previous frame. Concealed defects in the previous frame are included into the restoration procedure.

The obtained volume of $16 \times 16 \times 3$ is extended by zero padding to $16 \times 16 \times 16$ in order to be processed of a 3-D FFT. The other parameters remain unchanged.

4. RESULTS

Images from two different types of recordings are shown in Fig. 2 and Fig. 4 on the left hand side, respectively, including the error maps which are displayed on the right hand side of the respective figure. Only subjective visual results are shown. No objective measurements are done since PSNR is not of significance because medical images contain a lot of noise. The 2-D extrapolation algorithm is applied in order to restore defects in static radiographs. In contrary, in case of cine-angiography or fluoroscopy, additionally to spatial also temporal information is exploited by using the 3-D extrapolation algorithm. First, we show results applying the 2-D algorithm and then subsequently the results obtained by 3-D extrapolation.

In the following, the results obtained by 2-D extrapolation are described. In Fig. 3 and Fig. 5 on the left hand side, respectively, the results for the restored defects of all test images are displayed showing the excellent performance of the extrapolation algorithm. The error map is removed for all kinds of errors, no matter if cluster errors, the grid or row losses. For example, in Fig. 5 on the left hand side showing vascular angiography, different textures are restored, no matter if it is the smooth area of the background, edges like the restored vessel made visible by a contrast medium, or the filigree structures of the bone. Besides, the replacements appear naturally due to the imitation of noise which is very important.

The complexity is decreased significantly with approximately 5 iterations per block in contrary to [18] where 500 iterations per block are required. The better performance at the reduced complexity is due to the isotropic weighting function which allows to adapt better to the local surrounding because the influence of pixels on the extrapolation result decreases with distance to the defect.

Next, defects are restored by 3-D extrapolation. On average, only approximately 10 coefficients per block have to be estimated. The results are displayed in Fig. 3 and Fig. 5 on the right hand side, respectively. The 3-D extrapolation algorithm shows a similar excellent performance as the 2-D approach. Nevertheless, minor differences can be observed. In Fig. 3 on the right hand side, e.g., the restoration of the marked area appears closer to the original in Fig. 2 than the respective area in Fig. 3 on the left hand side obtained by 2-D extrapolation. This is achieved by involving additionally to spatial also temporal information.

5. CONCLUSION

We present a frequency selective extrapolation method in order to remove defects in X-ray imaging acquired by flat panel detectors. The medical image signal is extended into the defective area by evaluating the surrounding of the defect spectrally. Defects in static radiographs are concealed by 2-D extrapolation evaluating the spatial surrounding. The computational cost could be reduced significantly to a previous approach [18] by a better adaptation of the error criterion to the signal. In case of 3-D data as in cine-angiography or rotational volume sequences, the signal in a volume is extended by taking additionally to the spatial also the temporal surrounding into account by the 3-D extrapolation approach. The ability of inherent motion compensation is of great advantage since conventional motion compensation techniques known from video coding are difficult to apply due to the large amount of noise in medical image data. The frequency selective extrapolation method is able to restore smooth areas, edges as well as patterns. Even noise-like areas are restored which leads to a natural appearance.

6. REFERENCES

[1] T. Aach, U. Schiebel, and G. Spekowius, "Digital image acquisition and processing in medical X-ray imaging," *Journal of Electronic Imaging* **8**(Special Section on Biomedical Image Representation), pp. 7–22, 1999.

[2] J. A. Rowlands and J. Yorkston, "Flat panel detectors for digital radiography," in *Handbook of Medical Imaging*, J. Beutel, H. L. Kundel, and R. L. van Metter, eds., pp. 223–328, Springer Verlag, 2000.

[3] R. Guillemaud and L. Simon, "Evaluation of a fluoroscopy mode for a CCD-based radiographic detector," in *Medical Imaging 2000: Physics of Medical Imaging*, J. Dobbins and J. Boone, eds., pp. 137–144, SPIE Volume 3977, (Bellingham, Washington), February 2000.

[4] N. Jung, P. L. Alving, F. Busse, N. Conrads, H. M. Meulenbrugge, W. Rütten, U. Schiebel, M. Weibrecht, and H. Wieczorek, "Dynamic X-ray imaging system based on an amor-

phous silicon thin-film array," in *Physics of Medical Imaging*, vol. SPIE Vol. 3336, 1998.

[5] T. C. J. Bruijns, T. Adraansz, A. R. Cowen, A. G. Davies, S. M. Kengyelics, K. Kiani, H. Kroon, and H. Luijendijk, "Simulation of the quality of an a-Si flat X-ray detector system in low dose fluoroscopic applications," in *Medical Imaging 2000: Physics of medical Imaging*, J. Dobbins and J. Boone, eds., pp. 117–127, SPIE Volume 3977, (Bellingham, Washington), February 2000.

[6] M. Stahl, T. Aach, S. Dippel, T. Buzug, R. Wiemker, and U. Neitzel, "Noise-resistant weak-structure enhancement for digital radiography," in *SPIE Medical Imaging 99: Image Processing*, K. M. Hanson, ed., pp. 1406–1417, SPIE Vol. 3661, (San Diego, USA), February 20–26 1999.

[7] M. Stahl, T. Aach, and S. Dippel, "Digital radiography enhancement by nonlinear multiscale processing," *Medical Physics* **27**(1), pp. 56–65, 2000.

[8] G. Spekowius, H. Boerner, W. Eckenbach, P. Quadflieg, and G. J. Laurenssen, "Simulation of the imaging performance of X-ray image intensifier/ TV camera chains," in *Medical Imaging 1995*, pp. 12–23, (SPIE Vol. 2432), 1995.

[9] F. Xu, H. Liu, G. Wang, and B. A. Alford, "Comparison of adaptive linear interpolation and conventional linear interpolation for digital radiography systems," *Journal of Electronic Imaging* **9**(1), pp. 22–31, 2000.

[10] J. Hladuvka and E. Gröller, "Direction-Driven Shape-Based Interpolation of Volume Data," *Proceedings Vision, Modeling and Visualization*, pp. 113–120,521, Stuttgart, November 21–23 2001.

[11] F. S. Grassia. Practical parameterizations of rotations using the exponential map. *Journal of Graphics Tools,* 3(3):29–48, 1998

[12] T. Leung and J. Malik. Recognizing Surfaces using Three-Dimensional Textures. In *Int. Conf. on Computer Vision,* 1999, 32–46

[13] S. Upstill. *The RenderMan Companion.* Addison-Wesley, 1990

[14] A. Kaup, K. Meisinger, and T. Aach, "Frequency selective signal extrapolation with applications to error concealment in image communication," *Int. J. Electron. Commun. (AEÜ)*, vol. 59, pp. 147–156, June 2005.

[15] Meisinger, K.; Kaup, A.: Spatial error concealment of corrupted image data using frequency selective extrapolation. Proc. Int. Conf. on Acoustics, Speech, and Signal Processing (ICASSP), Montreal Canada, May 2004. 209–212.

[16] K. Meisinger and A. Kaup, "Minimizing a weighted error criterion for spatial error concealment of missing image data," in *Proc. Int. Conf. on Image Processing (ICIP)*, Singapore, Oct. 2004, pp. 813–816.

[17] K. Meisinger, S. Martin, and A. Kaup, "Spatio-temporal selective extrapolation for 3-D signals applied to concealment in video communications," in *Proc. European Signal Processing Conference*, Italy, Sep. 2006.

[18] Aach, T.; Metzler, V.: Defect interpolation in digital radiography - how object-oriented transform coding helps. Medical Imaging 2001, San Diego, USA, February 17–22 2001. Sonka, M.; Hanson, K. M. (eds.). SPIE Vol. 4322, 824–835.

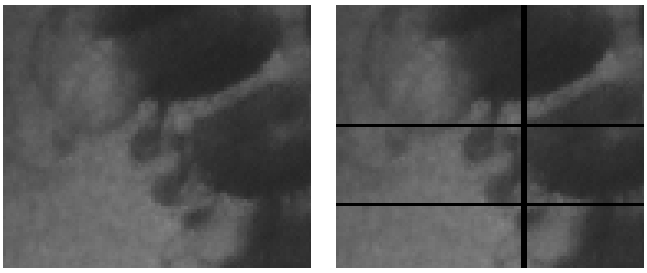

Fig. 2. Left: Part of original universal radiography/fluoroscopy sequence 'Colon'. Right: Part of defective sequence 'Colon'.

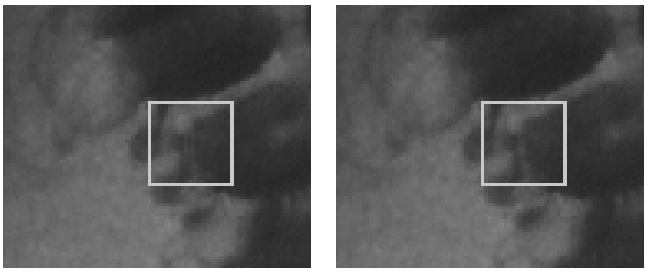

Fig. 3. Left: Restored by 2-D extrapolation. Right: Restored by 3-D extrapolation involving one previous and one following frame.

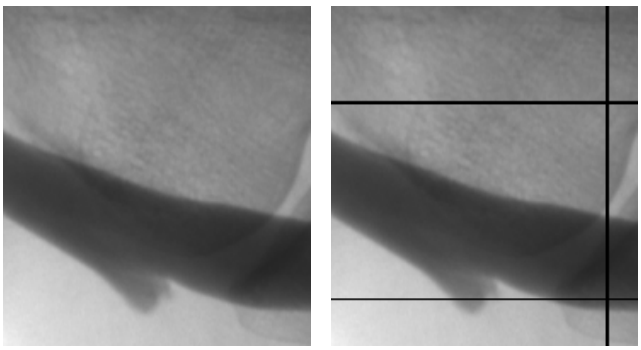

Fig. 4. Left: Part of original sequence 'Vascular Angiography'. Right: Part of defective sequence 'Vascular Angiography'.

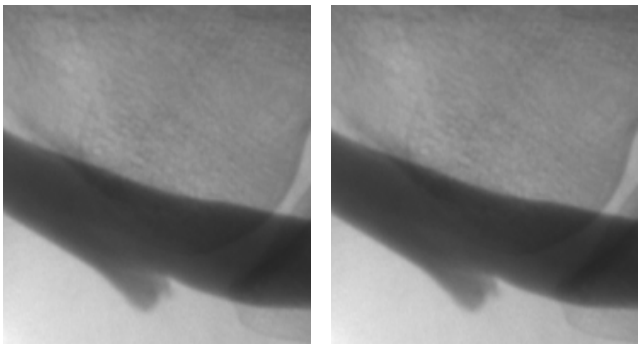

Fig. 5. Left: Restored by 2-D extrapolation. Right: Restored by 3-D extrapolation involving one previous and one following frame.